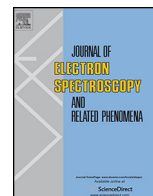




Contents lists available at ScienceDirect

## Journal of Electron Spectroscopy and Related Phenomena

journal homepage: [www.elsevier.com/locate/elspec](http://www.elsevier.com/locate/elspec)



# Photoelectron spectra and electronic structure of nitrogen analogues of boron $\beta$ -diketonates with aromatic substituents

Sergey A. Tikhonov<sup>a,\*</sup>, Vitaliy I. Vovna<sup>a</sup>, Aleksandr V. Borisenko<sup>b</sup>

<sup>a</sup> Far Eastern Federal University, 8 Sukhanova St., Vladivostok, 690950, Russia

<sup>b</sup> Vladivostok Branch of Russian Customs Academy, 16v Strelkovaya St., Vladivostok, 690034, Russia

### ARTICLE INFO

#### Article history:

Received 1 March 2016

Received in revised form

27 September 2016

Accepted 18 November 2016

Available online xxx

#### Keywords:

Electronic structure

Photoelectron spectra

Density functional theory

$\beta$ -Diketonates

Boron formazanates

### ABSTRACT

The electronic structure of three nitrogen analogues of boron  $\beta$ -diketonates containing aromatic substituents was studied by the ultraviolet photoelectron spectroscopy and within the density functional theory. In order to determine effects of heteroatom substitution in the chelate ligand, a comparative analysis was carried out for the electronic structure of three model compounds. In a range of model compounds, the HOMO's nature was revealed to be the same. The HOMO-1 orbital of nitrogen containing compounds is determined by the presence of lone electron pairs of nitrogen. In a range of the complexes under study, the influence of aromatic substituents on the electronic structure was defined. In the imidoylamidinate complex, in contrast to formazanates and  $\beta$ -diketonates, it was found the absence of any noticeable mixing of  $\pi$ -orbitals of the chelate and benzene rings. It was shown that within energy range to 11 eV, the calculated results reproduce well the energy differences between the ionized states of complexes.

© 2016 Elsevier B.V. All rights reserved.

## 1. Introduction

Boron chelate complexes possess important physico-chemical properties. In particular, boron  $\beta$ -diketonates ( $X_2B(O-C(R_1)-C(R_2)-C(R_3)-O)$ ) exhibit intensive luminescence [1–5], liquid crystal properties ( $X = F$ ) [6–8] and high biological activity ( $X = C_6H_5$ ) [9,10]. Boron  $\beta$ -diketonates are used as laser dyes [11], active components of solar collectors [12], materials for nonlinear optics [13] ( $X = F$ ) and antiviral drugs ( $X = C_6H_5$ ) [10].

Research of optical properties of nitrogen-containing analogues of boron  $\beta$ -diketonates causes also great interest [14–17]. Luminescent properties of boron imidoylamidates ( $X_2B(NH-C(R_1)-N-C(R_2)-NH)$ ) determine their application as laser dyes [18,19]. A special attention of researchers is attracted by the boron formazanates ( $X_2B(N(R_1)-N-C-N(R_2))$ ) that are relatively easily synthesized [20–23] and can be used to produce new phosphors in a broad spectral range [24–26].

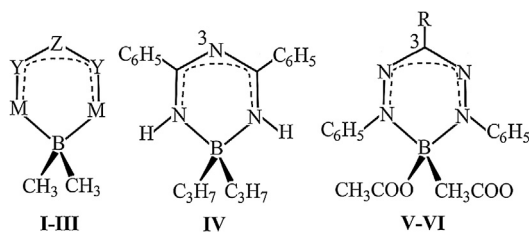
An introduction of substituents allows to control purposefully the optical properties of complexes, that determines the relevance of research on the relationship of the electronic structure and spectral characteristics of nitrogen analogues of boron  $\beta$ -diketonates.

Revealing relationships between functional characteristics of substances and their electronic structure opens opportunities for the controlled synthesis of new compounds with preassigned properties. Previously, we have published results on the electronic structure of some nitrogen analogues of boron  $\beta$ -diketonates studied by the methods of ultraviolet photoelectron spectroscopy (UPS) of vapor and the density functional theory (DFT) [27]. As we have shown in Refs. [28–30], the DFT calculations allow to estimate the ionization energy (IE) within an accuracy of 0.1 eV for boron complexes with aromatic substituents. Good agreement between theoretical and experimental data makes it possible to analyze the structure of the valence electron levels and interpret the photoelectron (PE) spectra unambiguously.

In order to determine the effect of substitution of heteroatoms in the chelate ligand, the data on the electronic structure were analyzed for the model compounds I–III. The obtained regularities were used in researches of the electronic structure of nitrogen-containing boron complexes IV–VI by the methods of UPS and DFT. Interpretations of the spectra were performed using the results of calculations.

\* Corresponding author.

E-mail addresses: [allser@bk.ru](mailto:allser@bk.ru), [tikhonov.sa@dvfu.ru](mailto:tikhonov.sa@dvfu.ru) (S.A. Tikhonov).



- I. M=O, Y=CH, Z=CH  
II. M=NH, Y=CH, Z=N  
III. M=NH, Y=N, Z=CH  
V. R=H  
VI. R=4-C<sub>6</sub>H<sub>4</sub>CH<sub>3</sub>

## 2. Experimental and calculation methods

The samples were synthesized within techniques described in Ref. [31] at the Institute of Organic Chemistry named after N.D. Zelinsky, RAS. PE spectra of vapors of the compounds IV–VI were obtained on a modified electronic spectrometer ES-3201 with a monochromatic light source He I ( $h\nu = 21.2$  eV). The spectral energy resolution is 0.08 eV, and it was determined by the width at half-maximum of the xenon peak. The temperature of the ionization cell was dependent on the temperature of vapor sublimation of a particular sample and was in the range from 180 to 240 °C. All spectra had bands in the range from 7 to 11 eV. In the range of energies above 11 eV, it was impossible to interpret spectra due to the high density of states.

Selecting the calculation method was based on the analogy between the quasi partial Dyson equation and the KS equation. The general Dyson equation [32] is one of the ways to obtain the Green's functions [33]. It was shown in Refs. [34,35] that in the valence range, the KS orbitals can be a good approximation to the Dyson orbitals. That explains the good correlation of experimental and theoretical IEs. The last statement was verified on the example of boron  $\beta$ -diketonates [28–30] and their nitrogen containing analogues [27]. A comparison of experimental and calculated data for IE of eleven boron  $\beta$ -diketonates has showed an average deviation of 0.06 eV for 79 levels [28–30]. For eleven nitrogen complexes the experimental  $IE_i$  and calculated energies  $\varepsilon_i$  are correlated with an accuracy of 0.1 eV [27].

**Table 1**  
Total effective charges NBO (e) and bond orders in the compounds I–III.

Compound	Effective charge					Bond orders			
	2CH <sub>3</sub>	B	2M	2Y	Z	B–C	B–M	M–Y	Y–Z
I	–0.57	0.81	–1.06	1.09	–0.27	0.99	0.70	1.51	1.39
II	–0.53	0.58	–0.50	1.05	–0.60	0.97	0.73	1.51	1.48
III	–0.51	0.53	0.03	–0.25	0.20	0.97	0.73	1.40	1.48

**Table 2**  
MO nature and symmetry, localization of electron density (%), calculated electron energies  $-\varepsilon_i$ , the energies of the Gaussian maximum  $IE_g$ , and the values  $\delta_i$  (eV) for the compound IV.

MO number, symmetry, nature	MO contributions			$-\varepsilon_i$	$IE_g$	$\delta_i$
	X	$\beta$	2C <sub>6</sub> H <sub>5</sub>			
HOMO, $b(\pi_3^{\beta}-\sigma''^X)$	51	48	1	5.83	7.59	1.76
HOMO-1, $b(\pi_3^{Ph})$	6	13	81	7.09	8.86	1.77
HOMO-2, $a(\pi_3^{Ph})$	2	22	76	7.17	8.92	1.75
HOMO-3, $a(\pi_2^{Ph})$	1	8	91	7.30	9.19	1.89
HOMO-4, $b(\pi_2^{Ph})$	0	1	99	7.33	9.23	1.90
HOMO-5, $a(n_N + \sigma''^X)$	24	60	16	7.57	9.44	1.87
HOMO-6, $b(\sigma''^X + \pi_3^{\beta})$	57	31	12	7.79	9.56	1.77
HOMO-7, $a(\sigma''^X + n_{\sigma}^{\beta})$	67	27	6	7.81	9.67	1.86

In our DFT quantum chemistry calculations, we applied the Firefly 7.1.G software program [36] using the tzvpp basic set [37,38]. The calculation results depend on type of exchange-correlation functional. At the present time the hybrid functionals [39], double-hybrid functionals [40], Minnesota functionals [41] and range-separated functionals [42–45] are used for DFT calculations. The method of dispersion correction as an add-on to standard Kohn-Sham density functional theory [46] is also used. In this paper, we study boron chelates built from H, B, C, N, and O atoms. The hybrid three-parameter functional B3LYP [47–49] are successfully used for DFT calculations of boron complexes. The goal of our research is the electronic structure in ground state and the interpretation of ultraviolet photoelectron spectra. In our review [30] it was shown that hybrid B3LYP functional [50–52] gives good results for investigation of electronic structure of boron complexes by UPS method. Because we used B3LYP functional in our previous researches [27–30], we used it in this paper too. This allows excluding the influence of functional type on the electronic effects of substitution.

In order to verify that the optimized structures match to the minimums on the potential energy surface, the Hessian was calculated. The absence of imaginary frequencies in the vibrational spectrum indicates an achievement of the energy minimum.

To compare the experimental values of vertical IEs with energies of the KS orbitals  $\varepsilon_i$ , the procedure was applied which was similar to the extended Koopman's theorem:

$$IE_i = -\varepsilon_i + \delta_i,$$

where  $IE_i$  is the energy of ionization;  $\varepsilon_i$  is the KS single-electron energy;  $\delta_i$  is a defect of the DFT approximation (DFA-defect) that is a measure of deviation of the calculated single-electron energies  $\varepsilon_i$  from the experimental vertical  $IE_i$ .

The bands in the UV PE spectra corresponding to several orbitals were decomposed into Gaussians. The energies of Gaussian maximums  $IE_g$  were considered as the  $IE_i$  values.

The predominant localization of MOs was denoted by indices in the text and tables: "X" – on the complexing agent (CH<sub>3</sub>)<sub>2</sub>B, (C<sub>3</sub>H<sub>7</sub>)<sub>2</sub>B, (CH<sub>3</sub>COO)<sub>2</sub>B; " $\beta$ " – on the ligand O–C–C–O, NH–C–N–C–NH, N–N–C–N–N; "Ph" – on the benzene ring C<sub>6</sub>H<sub>5</sub>; "R" – on the substituents (H, 4-C<sub>6</sub>H<sub>4</sub>CH<sub>3</sub>). For BC<sub>2</sub> and BO<sub>2</sub>-bonding orbitals ( $\sigma^X$ ), the local C<sub>s</sub> symmetry was used relative to the chelate ligand plane.

**Table 3**

MO nature and symmetry, localization of electron density (%), calculated electron energies  $-\varepsilon_i$ , the energies of the Gaussian maximum  $IE_g$ , and the values  $\delta_i$  (eV) for the compounds V–VI.

MO number, symmetry, nature	MO contributions				$-\varepsilon_i$	$IE_g$	$\delta_i$
	X	$\beta$	2C <sub>6</sub> H <sub>5</sub>	R			
Compound V							
HOMO, $b(\pi_3^{\text{Ph}}-\pi_3^{\beta})$	3	43	54	0	6.33	8.32	1.99
HOMO-1, $b(\pi_2^{\text{Ph}}-\sigma^{\text{X}})$	36	11	53	0	6.97	9.07	2.10
HOMO-2, $a(\pi_3^{\text{Ph}}-\sigma^{\text{X}})$	29	2	69	0	7.05	9.33	2.28
HOMO-3, $a(\pi_2^{\text{Ph}})$	5	7	88	0	7.22	9.37	2.15
HOMO-4, $b(\sigma^{\text{X}}-\pi_2^{\text{Ph}})$	53	3	44	0	7.33	9.47	2.14
HOMO-5, $a(\sigma^{\text{X}}-\pi_2^{\text{Ph}})$	65	3	32	0	7.42	9.7	2.28
HOMO-6, $b(n_{\beta}+\sigma^{\text{X}})$	21	59	20	0	7.53	9.78	2.25
HOMO-7, $b(\pi_3^{\text{Ph}}+\pi_3^{\beta})$	14	41	45	0	8.06	10.12	2.06
Compound VI							
HOMO, $b(\pi_3^{\text{R}}-\pi_3^{\beta})$	3	38	20	39	5.79	7.84	2.05
HOMO-1, $b(\pi_2^{\text{Ph}}-\sigma^{\text{X}})$	27	10	48	15	6.91	9.20	2.29
HOMO-2, $a(\pi_2^{\text{R}})$	4	4	20	72	6.99	9.30	2.31
HOMO-3, $b(\pi_2^{\text{Ph}}-\pi_2^{\text{R}})$	6	12	45	37	7.00	9.30	2.30
HOMO-4, $a(\pi_2^{\text{Ph}}-\sigma^{\text{X}})$	26	1	62	11	7.05	9.42	2.37
HOMO-5, $a(\pi_2^{\text{Ph}})$	5	7	86	2	7.22	9.58	2.36
HOMO-6, $b(\pi_2^{\text{Ph}}-\sigma^{\text{X}})$	38	9	51	2	7.34	9.70	2.36
HOMO-7, $a(\sigma^{\text{X}}-\pi_2^{\text{Ph}})$	66	3	31	0	7.42	9.80	2.38
HOMO-8, $b(n_{\beta}+\sigma^{\text{X}})$	41	47	6	6	7.45	9.85	2.40
HOMO-9, $b(\pi_3^{\beta}+\pi_3^{\text{Ph}}+\pi_3^{\text{R}})$	8	36	33	23	8.20	10.40	2.20

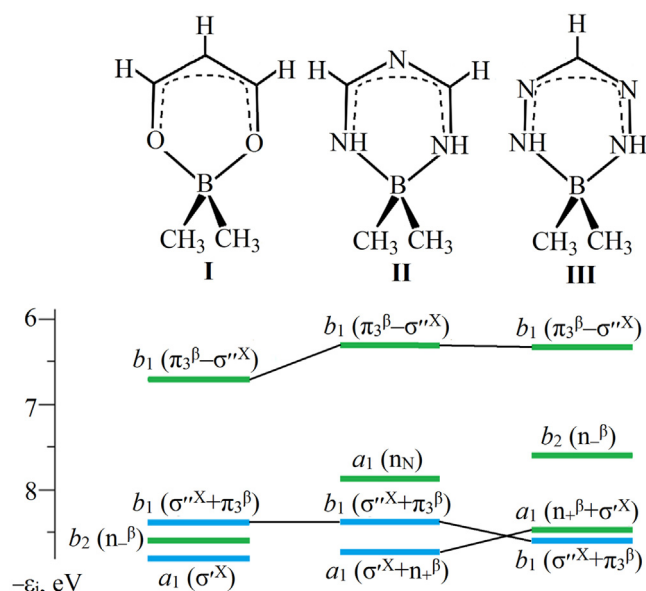


**Fig. 1.** Correlation diagram for the four highest occupied  $\pi$ - and  $\sigma$ -MOs of the model compounds I–III. The predominant localization is shown by colors: green – the chelating ligand  $\beta$ , blue – the complexing agent X. (For interpretation of the references to colour in this figure legend, the reader is referred to the web version of this article.)

### 3. Results and discussion

In order to determine the effect of substitution of heteroatoms in the chelate ligand, analysis of calculated data on the electronic structure was performed for three isoelectronic analogues: acetylacetonate (I), imidoylamidinate complex (II), and formazanate (III) (Fig. 1). All three compounds have the  $C_{2v}$  symmetry.

According to analysis of the geometry optimization results, there are only little changes in the structural parameters (Table 1) in a series of complexes I–III. In contrast to the compounds II and III, in the complex I, the boron atom gives up electron density to the chelating ligand. The atoms 2Y in compounds I–II are electron donors for atoms 2M and Z (Table 1). In the compound III, atoms Z are electron donors for atoms 2Y.

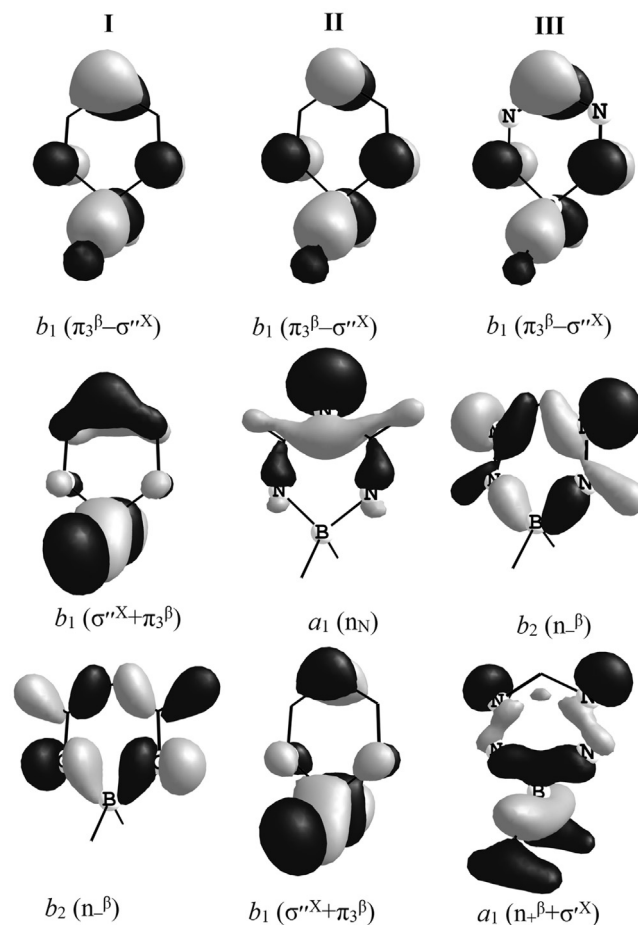


**Fig. 2.** The shape of three highest occupied MOs in the model compounds I–III.

The highest occupied molecular orbital (HOMO)  $\pi_3^{\beta}$  of the compounds I–III is mixed with the MO  $\sigma^{\text{X}}$  (Figs. 1, 2). The difference in energy of the levels  $\pi_3^{\beta}-\sigma^{\text{X}}$  and  $\sigma^{\text{X}}+\pi_3^{\beta}$  is of 1.67 (I), 2.05 (II), and 2.25 (III) eV. Higher splitting of the  $\pi_3^{\beta}$  level in the nitrogen containing compounds II and III is caused by the influence of nitrogen  $n$ -orbitals (Figs. 1, 2). In the complex II, the HOMO-1 is

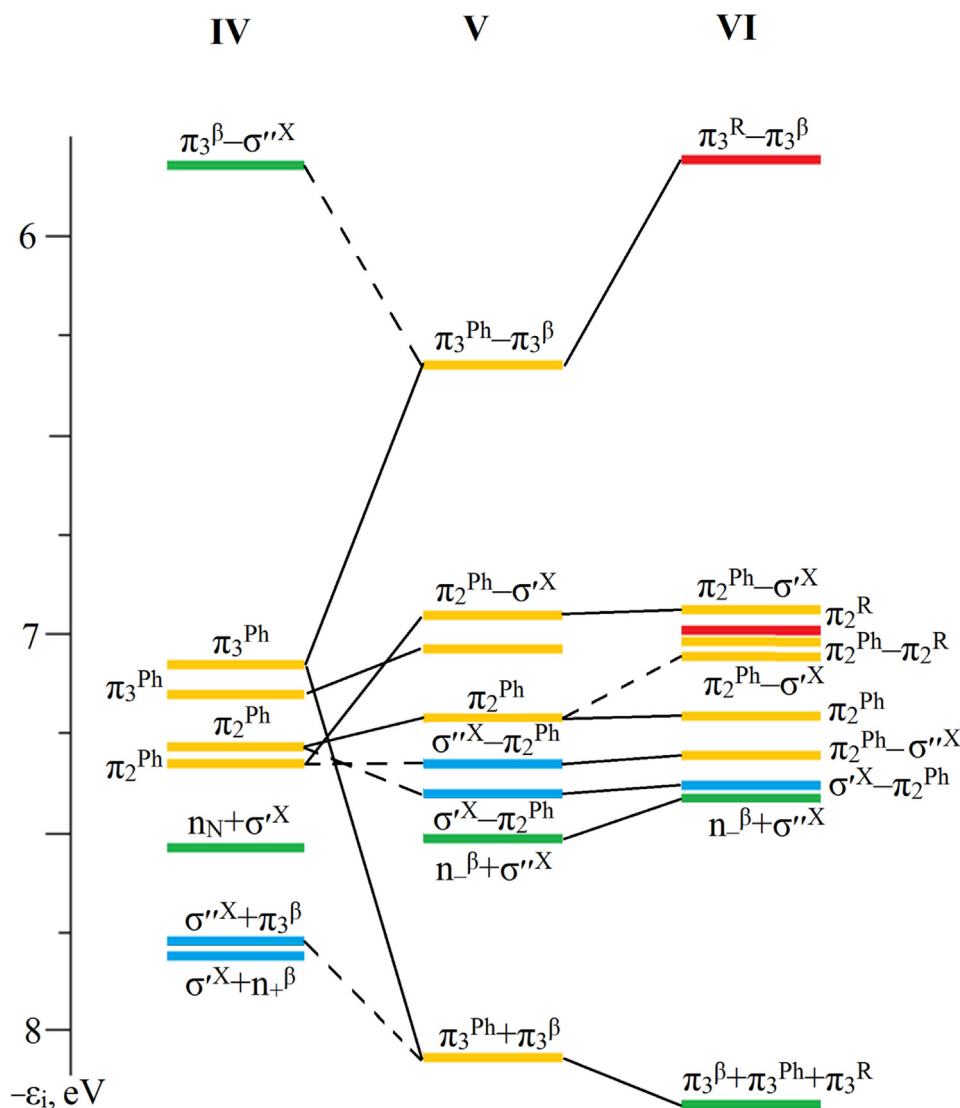


**Fig. 3.** Correlation diagram for the highest occupied  $\pi$ - and  $\sigma$ -MOs of the compounds IV–VI. The predominant localization is shown by colors: green – the chelating ligand  $\beta$ , blue – the complexing agent X, orange – the phenyl rings Ph, red – the substituent R. (For interpretation of the references to colour in this figure legend, the reader is referred to the web version of this article.)

predominantly localized on the nitrogen atom in  $\gamma$ -position (Fig. 2), that is determined by the presence of lone electron pair (LEP). The HOMO-1 in the compound III is localized on four nitrogen atoms. In complexes II and III, the  $n_{+}^{\beta}$  orbital is mixed with the orbital of complexing agent  $\sigma'^X$  (Figs. 1, 2).

The highest occupied electronic levels of  $\beta$ -diketonate complex (I) and boron dimethyl formazanate (III) are similar in the nature (Figs. 1, 2). The difference in energy of the levels  $\pi_3^{\beta}-\sigma''^X$  and  $n_{-}^{\beta}$  in the compounds I and III is of 0.47 and 1.10 eV (Fig. 1).

According to the results of geometry optimization, the molecule IV is symmetrical about the axis of the second order passing through the atoms B and N3. A minimum of the total energy is observed when  $C_2H_5$  fragments of the complexing agent are located on both sides from a plane, which is perpendicular to the chelate ring. The dihedral angles between the planes of the chelate and benzene rings are equal  $25^\circ$ .

According to calculations, the molecule V is symmetrical about the axis of the second order passing through atoms B and C3. The structure of the compound VI is close to  $C_2$  symmetry. In the compound VI, the chelate ring and the substituent  $C_6H_4CH_3$  are located in one plane. The dihedral angles between the planes of the chelate

and benzene rings are equal  $46^\circ$  (compound V) and  $47^\circ$  (complex VI).

In the complex IV, there is no any noticeable mixing of the MOs  $\pi_3^{\beta}$  and  $\pi_3^{Ph}$  (Table 2). The presence of four orbitals of the benzene rings does not cause a noticeable change in the energy difference between the levels  $\pi_3^{\beta}-\sigma''^X$  and  $\sigma''^X+\pi_3^{\beta}$  compared to the model compound II (Fig. 1, Table 2). The influence of propyl groups causes the MO energies stabilization by 0.2–0.8 eV.

In the complexes V and VI, in contrast to IV, there is a noticeable mixing of  $\pi$ -orbitals of the ligand and the MOs of benzene rings (Table 3, Figs. 3–4), which is characteristic for the boron  $\beta$ -diketonates [28,29]. The mixing of orbitals leads to stabilizing the highest occupied MO of the complex V by 0.50 eV and to splitting of the level  $\pi_3^{Ph}$  (Fig. 3, Tables 2, 3). The calculated difference of the MO energies  $\pi_3^{Ph}-\pi_3^{\beta}$  and  $\pi_3^{Ph}+\pi_3^{\beta}$  is equal 1.73 eV (Fig. 3, Table 3). The mixing of the MO  $\pi_2^{Ph}$  with the orbital  $\sigma'^X$  leads to destabilization of the levels  $\pi_2^{Ph}$  by 0.1–0.3 eV (Fig. 3, Tables 2, 3).

The presence of  $C_6H_4CH_3$  group as a substituent (complex VI) leads to a significant delocalization of MO (Table 3). The mixing of the orbital  $\pi_3^{\beta}$  the MO  $\pi_3^R$  leads to destabilization of the electron energies of the highest occupied molecular orbital by 0.53 eV

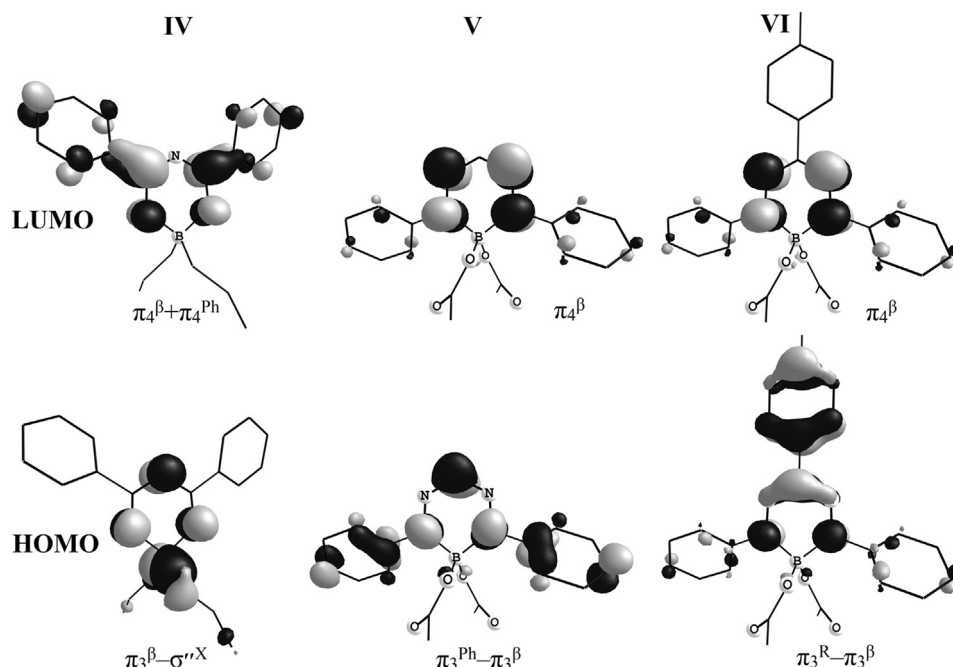


Fig. 4. HOMO and LUMO of compounds IV–VI.

Table 4

The total effective charges NBO of the complexing agent and chelate ligand, bond orders in the first coordination sphere in the compounds IV–VI.

Compound	Effective charge				Bond orders	
	X	$\beta$	2Ph	R	B–N	B–X
IV	0.04	–0.11	0.07	–	0.76	0.95
V	0.06	–0.76	0.5	0.2	0.81	0.99
VI	0.07	–0.56	0.52	–0.03	0.80	0.99

(Figs. 3–4, Table 3). The influence of the additional  $\pi$ -MOs of the substituent  $\text{C}_6\text{H}_4\text{CH}_3$  causes an increase in splitting of the level  $\pi_3^\beta$  by 0.69 eV (Fig. 3, Table 3).

The effective charges NBO and bond orders B–N and B–X, listed in Table 4, indicate the influence of substituents on the electron density distribution in the fragments of molecules and on covalent binding in the first coordination sphere. In the studied complexes, charges of the complexing agents X are close to zero (Table 4). The boron atom charge in the complex IV is equal +0.63 e, in the complexes V and VI it is equal +1.04 e. The ionic character of B–X bonds is more noticeable in the complexes V and VI, that is explained by the acceptor properties of two oxygen atoms (–1.40 e). The charges of the chelate ligand and benzene rings are the most different in the boron formazanates V and VI (Table 4). The bond orders in B–N and B–X in a series of compounds IV–VI vary slightly (Table 4).

An increase in  $\text{IE}_1$  by 0.73 eV (Fig. 5) at transition from IV–V is mainly caused by the field effect of two acceptor groups  $\text{CH}_3\text{COO}$  (–0.98 e). An addition of  $\text{C}_6\text{H}_4\text{CH}_3$  group stabilizes IE of HOMO by 0.48 eV. By analogy with  $\beta$ -diketonate complexes [28–30] the HOMO bands have broad contours in UPS spectra of IV–VI compounds (Fig. 5). The first band shape in the UPS spectra of IV–VI is defined by a set of components for 3N–6 vibrations. Significant changes in the equilibrium coordinate values of stretching and deformation vibrations in the ion, according to the Franck–Condon principle, cause an excess at 0.58–0.87 eV of the vertical transition energy over the adiabatic one. The maximum width of the first band is observed for the spectrum V, that is caused by the HOMO delocalization into three cycles (Fig. 4).

When removing electrons from the binding MOs, the vibrational contours of bands are asymmetrical [53]. The asymmetric shapes of Gaussian components are observed in spectra of the studied compounds (Fig. 5), that is also characteristic for the  $\pi$ - and  $n$ -MOs of benzene molecules [54], heterocycles [55],  $\beta$ -diketonate complexes of boron and their analogues containing nitrogen [27–30]. The asymmetry parameter value of the first band (the ratio of the left/right values of half-width) for IV and VI are 1.12 and 1.10, respectively. In the substance V there is an overlap of the first and second spectral bands, making it difficult to define the asymmetry parameter. According to the deconvolution, the first band in the spectrum V is symmetric (Fig. 5).

According to the calculations, the first band in the compound IV spectrum corresponds to the MO  $\pi_3^\beta\text{--}\sigma^{\text{R}^{\text{X}}}$  (Fig. 5, Table 2). The second band in the PE spectrum of the compound IV corresponds to seven MOs, including four orbitals localized mainly on the benzene rings (Fig. 5, Table 2). The spectral region at 10 eV (Fig. 5) is associated with orbitals localized mainly on the propyl groups.

The first band in the compound V spectrum corresponds to the MO  $\pi_3^{\text{Ph}}\text{--}\pi_3^\beta$  (Figs. 5, Table 3). The second band of the compound V spectrum corresponds to seven MOs. Increasing the spectrum intensity at 11 eV is caused by processes of photoionization from the MO  $\sigma^{\text{R}^{\text{X}}}$ .

The maximum in the complex VI spectrum at 7.8 eV is associated with the orbital  $\pi_3^{\text{R}}\text{--}\pi_3^\beta$  (Fig. 5, Table 3). Then two overlapping bands are observed, which correspond to seven and three MOs. The spectrum region at 12 eV corresponds to the MOs  $n_4^\beta\text{--}\sigma^{\text{R}}$  and  $\sigma^{\text{R}}$ .



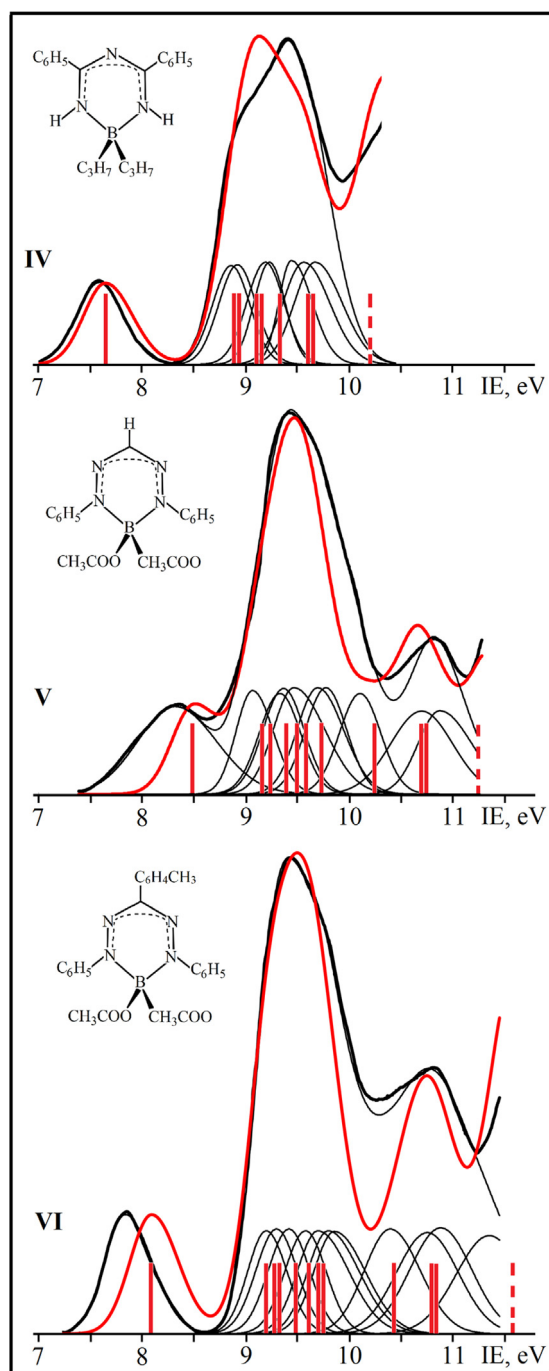


**Fig. 5.** Ultraviolet photoelectron spectra of vapors of the compounds IV–VI (thick line). The bands in the UPS spectra corresponding to several orbitals were decomposed into Gaussians (thin envelope line). When decomposing the spectral bands into Gaussians, the following characteristics were taken into account: the number of calculated electronic levels, energy difference between them, and the proximity of their ionization cross sections. The vertical red lines in the spectra correspond to the calculated values of electron energies shifted by the value of the average DFA-defect. The dashed red lines indicate the next calculated electron levels, which IEs have not been determined. The theoretical spectra are shown in red. The relative cross-sections for components (the asymmetry parameter is 1.10) of DFT spectra with the predominant contribution of oxygen and nitrogen AOs are 20% less than the corresponding values for carbon orbitals. The width at half-maximum for all components of the DFT spectra is 0.55 eV. (For interpretation of the references to colour in this figure legend, the reader is referred to the web version of this article.)

## 4. Conclusion

The substitution of heteroatoms in the chelate ligand does not change the HOMO nature in a series of the model compounds. The lone electron pairs of nitrogen atoms control the HOMO-1 nature in the compounds II and III, that causes an increase in the energy difference between the MOs  $\pi_3^\beta - \sigma^{*X}$  and  $\sigma^{*X} + \pi_3^\beta$ .

Analysis of interaction of  $\pi$ -systems of the chelate ring and substituents in a series of compounds under study has shown mixing the orbitals  $\pi_3^\beta$  and  $\sigma^{*X}$ . In the imidoylamidinate complex, there is no any mixing the MOs  $\pi_3^\beta$  и  $\pi_3^{\text{Ph}}$ , which is characteristic for boron  $\beta$ -diketonates and formazanates. The introduction of the substituent  $\text{C}_6\text{H}_4\text{CH}_3$  in  $\gamma$ -position leads to a noticeable increase in splitting of the level  $\pi_3^\beta$ .

In the compounds IV, V, and VI, the average values of the DFA-defect are 1.82, 2.17, and 2.30 eV, respectively. Due to effects of the electron shell relaxation in the complexes IV and V, the value of DFA-defect for the HOMO is equal to 1.99 and 2.05 eV. In the series of compounds IV–VI, the maximum discrepancy between the experimental and theoretical IE for remaining 29 levels is equal 0.12 eV.

The obtained data can be used for development of new optical functional materials based on boron compounds, which are promising for devices of converting and processing of optical signals, optical sensors, and optoelectronics.

## References

- [1] S. Chibani, A. Charaf-Eddin, B. Mennucci, B.L. Guennic, D. Jacquemin, *J. Chem. Theory Comput.* 10 (2014) 805–815.
- [2] S.A. Tikhonov, V.I. Vovna, N.A. Gelfand, I.S. Osmushko, E.V. Fedorenko, A.G. Mirochnik, *J. Phys. Chem. A* 120 (2016) 7361–7369.
- [3] M.V. Kazachek, I.V. Svistunova, *Spectrochim. Acta, A* 148 (2015) 60–65.
- [4] W.A. Morris, T. Liu, C.L. Fraser, *J. Mater. Chem. C* 3 (2015) 352–363.
- [5] L. Wang, K. Wang, B. Zou, K. Ye, H. Zhang, *Y. Wang, Adv. Meter.* 27 (2015) 2918–2922.
- [6] M.J. Mayoral, P. Ovejero, M. Cano, G. Orellana, *Dalton Trans.* 40 (2011) 377–383.
- [7] I. Sánchez, J.A. Campo, J.V. Heras, M. Cano, E. Oliveira, *Inorg. Chim. Acta* 381 (2012) 124–136.
- [8] E. Gizirolu, A. Nesrullajev, N. Orhan, *J. Mol. Struct.* 1056 (2014) 246–253.
- [9] A. Flores-Parra, R. Contreras, *Coord. Chem. Rev.* 196 (2000) 85–124.
- [10] S.J. Baker, T. Akama, Y.K. Zhang, et al., *Bioorg. Med. Chem. Lett.* 16 (2006) 5963–5967.
- [11] P. Czerney, G. Haucke, C. Igney//Ger (East) DD/-265266. 1987. CA. 1990. V. 112. № 45278.
- [12] M. Halik, G. Schmid, L. Davis//German patent 10152938. CA. 2003. V. 123. № 378622.
- [13] R. Kammiller, G. Bourhill, Y. Jin, C. Bräuchle, G. Görlitz, H. Hartmann, *J. Chem. Soc., Faraday Trans.* 92 (1996) 945–947.
- [14] Y. Kubota, Y. Sakuma, K. Funabiki, M. Matsui, *J. Phys. Chem. A* 118 (2014) 8717–8729.
- [15] R. Yoshii, A. Hirose, K. Tanaka, Y. Chujo, *Chem. Eur. J.* 20 (2014) 8320–8324.
- [16] S.M. Barbon, J.T. Price, P.A. Reinkeluers, J.B. Gilroy, *Inorg. Chem.* 53 (2014) 10585–10593.
- [17] S. Knippenberg, M.V. Bohnwagner, P.H.P. Harbach, A. Dreuw, *J. Phys. Chem. A* 119 (2015) 1323–1331.
- [18] J. Banuelos, F.L. Arbeloa, V. Martinez, M. Liras, A. Costela, I.G. Moreno, I.L. Arbeloa, *Phys. Chem. Chem. Phys.* 13 (2011) 3437–3445.
- [19] Y. Deng, Y.-Y. Cheng, H. Liu, J. Mack, H. Lu, L.-G. Zhu, *Tetrahedron Lett.* 55 (2014) 3792–3796.
- [20] G.I. Sigeikin, G.N. Lipunova, I.G. Pervova, *Russ. Chem. Rev.* 75 (2006) 885–900.
- [21] D.E. Berry, R.G. Hicks, J.B. Gilroy, *J. Chem. Educ.* 86 (2009) 76–79.
- [22] M.-C. Chang, E. Otten, *Chem. Commun.* 50 (2014) 7431–7433.
- [23] S.M. Barbon, J.T. Price, U. Yogarajah, J.B. Giloy, *RSC Adv.* 69 (2015) 56316–56324.
- [24] S.M. Barbon, V.N. Staroverov, J.B. Gilroy, *J. Org. Chem.* 80 (2015) 5226–5235.
- [25] M. Hesari, S.M. Barbon, V.N. Staroverov, Z. Ding, J.B. Gilroy, *Chem. Commun.* 51 (2015) 3766–3769.
- [26] R.R. Maar, S.M. Barbon, N. Sharma, H. Groom, L.G. Luyt, J.B. Gilroy, *Chem. A Eur. J.* 21 (2015) 15589–15599.
- [27] S.A. Tikhonov, V.I. Vovna, *J. Struct. Chem.* 56 (2015) 446–453.
- [28] V.I. Vovna, S.A. Tikhonov, M.V. Kazachek, I.B. Lvov, V.V. Korochentsev, E.V. Fedorenko, A.G. Mirochnik, *J. Electron. Spectr. Relat. Phenom.* 189 (2013) 116–121.
- [29] V.I. Vovna, S.A. Tikhonov, I.B. Lvov, I.S. Osmushko, I.V. Svistunova, O.L. Shcheka, *J. Electron. Spectr. Relat. Phenom.* 197 (2014) 43–49.

- [30] I.S. Osmushko, V.I. Vovna, S.A. Tikhonov, Y.V. Chizhov, I.V. Krauklis, *Int. J. Quantum Chem.* 116 (2016) 325–332.
- [31] B.M. Mikhailov, V.A. Dorokhov, V.I. Seredenko, *Russ. Chem. Bull.* (1980) 485–491.
- [32] E.K.U. Gross, E. Runge, O. Heinonen, *Many Particle Theory*, Adam Hilger, 1992, pp. 418.
- [33] E.N. Economou, *Green's Functions in Quantum Physics*, Springer, New York, 1979, pp. 251.
- [34] S. Hamel, P. Duffy, M.E. Casida, D.R. Salahub, *J. Electron. Spectr. Relat. Phenom.* 123 (2002) 345–363.
- [35] P. Duffy, D.P. Chong, M.E. Casida, D.R. Salagub, *Phys. Rev. A* 50 (1994) 4707–4728.
- [36] A.A. Granovsky, Firefly version 7.1. G, <http://classic.chem.msu.su/gran/firefly/index.html>.
- [37] Basis Set Exchange. Version 1.2.2: <https://bse.pnl.gov/bse/portal>.
- [38] K. Eichkorn, F. Weigend, O. Treutler, R. Ahlrichs, *Theor. Chem. Acc.* 97 (1997) 119–124.
- [39] M. Marsman, J. Paier, A. Stroppa, G. Kresse, *J. Phys. Condensed Matter* 20 (2008) 064201.
- [40] L. Goerigk, S. Grimme, *Wiley Interdiscip. Rev.: Comput. Mol. Sci.* 6 (2014) 576–600.
- [41] Y. Zhao, D.G. Truhlar, *Chem. Phys. Lett.* 502 (2011) 1–13.
- [42] A.E. Raeber, B.M. Wong, *J. Chem. Theory Comput.* 11 (2015) 2199–2209.
- [43] A. Prlj, B.F.E. Curchod, A. Fabrizio, L. Floryan, C. Corminboeu, *J. Phys. Chem. Lett.* 6 (2015) 13–21.
- [44] L. Kronik, T. Stein, S. Refaely-Abramson, R. Baer, *J. Chem. Theory Comput.* 8 (2012) 1515–1531.
- [45] D.A. Egger, S. Weissman, S. Refaely-Abramson, S. Sharifzadeh, M. Dauth, R. Baer, S. Kümmel, J.B. Neaton, E. Zojer, L. Kronik, *J. Chem. Theory Comput.* 10 (2014) 1934–1952.
- [46] S. Grimme, J. Antony, S. Ehrlich, H. Krieg, *J. Chem. Phys.* 132 (2010) 154104–154118.
- [47] S. Ogawa, M. Morikawa, G. Juhasz, N. Kimizuka, *RSC Adv.* 5 (2015) 60373–60379.
- [48] Y. Kubota, K. Kasatani, H. Takai, K. Funabiki, M. Matsui, *Dalton Trans.* 44 (2015) 3326–3341.
- [49] M.-C. Chang, E. Otten, *Inorg. Chem.* 54 (2015) 8656–8664.
- [50] C. Lee, W. Yang, R.G. Parr, *Phys. Rev. B* 37 (1988) 785–789.
- [51] A.D. Becke, *J. Chem. Phys.* 98 (1993) 5648–5652.
- [52] P.J. Stevens, F.J. Devlin, C.F. Chablowski, M.J. Frisch, *J. Phys. Chem.* 98 (1994) 11623–11627.
- [53] S. Hüfner, *Photoelectron Spectroscopy: Principles and Applications*, Springer, Berlin, 1996.
- [54] L. Asbrink, O. Edqvist, E. Lindholm, L.E. Selin, *Chem. Phys. Lett.* 4 (5 N) (1970) 192–194.
- [55] W.V. Niessen, W.P. Kraemer, G.H.F. Diercksen, *Chem. Phys.* 41 (1979) 113–132.